International Journal of Engineering & Technology
ISSN: 3083-9114
Journal homepage: https://e-journal.scholar-publishing.org/index.php/ijet

Performance Evaluation of Nanoparticle-Based Coatings for Enhanced Protection and Surface Improvement of Metallic Materials

Muhammad Faisal[1], Iqbal[1], Muhtadin[1], Erdiwansyah[2], Mahyuddin[1], Muhibbuddin[3]

[1]Department of Mechanical Engineering, Universitas Abulyatama Aceh, Aceh Besar, 23372, Indonesia
[2]Department of Natural Resources and Environmental Management, Universitas Serambi Mekkah, Banda Aceh, 23245, Indonesia
[3]Department of Mechanical and Industrial Engineering, Universitas Syiah Kuala, Banda Aceh, 23111, Indonesia

Corresponding Author: faisal_mesin@abulyatama.ac.id

Abstract
Nanoparticle-based coatings offer enhanced protection and functional improvement for metallic materials; however, their performance is strongly influenced by the thermal–fluid conditions within the deposition system. This study aims to evaluate how variations in deposition column geometry and biomass fuel type affect temperature distribution, gas velocity, and radiative heat flux within a nanoparticle coating environment. A computational fluid dynamics (CFD) approach was applied using the schematic configuration of a 2160 mm vertical deposition column. Four geometries and three biomass fuels, palm kernel shell (PKS), Oil palm fronds (OPF), and empty fruit bunch (EFB), were analysed under identical boundary conditions. The governing conservation equations were solved alongside the Discrete Ordinates (DO) radiation model to capture temperature, velocity, and irradiation behaviour throughout the column. The results show that Geometry 3 produced the highest temperature field, reaching 2020 °C, while Geometry 4 exhibited favourable flow momentum, with peak velocities of 20 m/s. Geometry 1 and Geometry 2 showed moderate thermal and flow distributions, with maximum temperatures of 1875 °C and 1950 °C, respectively. Biomass fuel analysis revealed that PKS and EFB generated significantly higher thermal and radiative outputs, with irradiation values approaching 6.5 × 10^6 W/m², compared to PKS, which remained around 3.0 × 10^6 W/m². These findings demonstrate the novelty of integrating geometric optimisation with biomass combustion analysis to improve nanoparticle activation and coating uniformity. Overall, the study concludes that selecting an appropriate column geometry combined with high-performing biomass fuels can substantially enhance coating efficiency, offering a sustainable alternative to fossil-fuel-based systems.

Article Info
Received: 13 March 2025
Revised: 15 March 2025
Accepted: 26 March 2025
Available online: 30 March 2025

Keywords
Nanoparticle-based coatings
Biomass combustion
CFD simulation
Deposition column geometry
Radiative heat flux

1. Introduction

Nanoparticle-based coatings have become one of the most promising technologies for improving the protection, durability, and functional performance of metallic materials. Their ability to form nanoscale surface layers enables significant enhancements in corrosion resistance, thermal stability, and

mechanical strength. Numerous studies have demonstrated the advantages of nanoparticle coatings across automotive, aerospace, and energy applications, particularly when compared to conventional coating techniques that offer limited microstructural control (Erdiwansyah, Mahidin, et al., 2019; Han et al., 2020; Tang et al., 2018). Despite these advancements, the precise control of deposition environments remains a critical challenge that directly influences coating quality.

The deposition column plays a central role in determining the thermal, fluid, and radiative conditions under which nanoparticles are synthesised and deposited. Prior research has shown that temperature uniformity and flow turbulence within coating chambers strongly affect nanoparticle crystallisation, agglomeration behaviour, and adhesion properties (Erdiwansyah, Mamat, Sani, & Sudhakar, 2019; Rukosuyev, Barannyk, Oshkai, & Jun, 2016; Xing et al., 2019). However, many existing studies rely on simplified or idealised reactor geometries that do not fully capture the complex spatial variations in industrial-scale systems. This gap highlights the need for more detailed investigations into how geometric configurations influence coating performance.

In parallel, the growing interest in renewable energy systems has motivated researchers to explore biomass-derived heat sources for advanced material processing. Biomass fuels such as coconut shell, palm kernel shell, and empty fruit bunch are abundantly available in many tropical regions and have been extensively studied for combustion, gasification, and thermal energy applications (Gani et al., 2021; Liu et al., 2019; Radenahmad et al., 2020). Their combustion characteristics, particularly temperature output, combustion stability, and radiation intensity, make them potential alternatives to fossil fuels for high-temperature applications. However, their use in nanoparticle coating systems remains largely unexplored.

The integration of biomass fuels with nanoparticle-coating technologies offers a unique opportunity to develop sustainable, energy-efficient processes. Previous research has shown that biomass combustion can generate substantial radiative heat flux, which is valuable for assisting nanoparticle formation and thermal activation (El-Sayed, Mostafa, Khass, Noseir, & Ismail, 2024; Mahidin et al., 2022; Mohanna et al., 2021; Zheng et al., 2020). Yet, the interaction among fuel type, column geometry, and deposition behaviour has not been thoroughly examined, leaving significant uncertainties about the optimal conditions for coating uniformity and process stability.

Computational fluid dynamics (CFD) has emerged as a powerful tool for evaluating thermal–fluid processes in coating systems. CFD enables detailed simulation of temperature fields, gas velocities, and radiative heat transfer within complex geometries, providing insights that are difficult to obtain experimentally (Erdiwansyah et al., 2026; Erdiwansyah, Gani, et al., 2023; Erdiwansyah, Mahidin, et al., 2023; Håkansson, 2020). The Discrete Ordinates (DO) radiation model has proven effective in capturing radiative phenomena within high-temperature reactors. Despite its relevance, limited studies have applied CFD and DO radiation models to biomass-fuel-driven coating systems.

Given these knowledge gaps, there is a substantial need for integrated studies that combine geometric optimisation, biomass combustion analysis, and multiphysics CFD modelling. Such an approach would allow researchers to understand not only the behaviour of nanoparticles during deposition but also how system design and fuel choice affect heat transfer and flow conditions. This holistic perspective is essential for developing next-generation coating technologies that are both high-performance and environmentally sustainable.

The primary objective of this research is to evaluate how variations in deposition column geometry and biomass fuel type influence the temperature distribution, gas velocity profiles, and radiative heat flux within a nanoparticle coating system. By integrating the schematic configuration shown in **Fig. 1** with multiphysics CFD simulations, this study aims to identify the geometric and thermal–fluid conditions that most effectively promote uniform nanoparticle activation, stable transport, and enhanced coating quality. The findings aim to provide a scientific foundation for the development of sustainable, biomass-powered coating technologies with optimised thermal and flow performance.

2. Methodology

The research methodology adopted in this study was structured around the operational framework illustrated in the schematic diagram of the coating deposition column shown in **Fig. 1**. The system consists of three primary zones, namely the lower combustion chamber (0 mm reference point), the central coating or reaction zone, and the upper exhaust section (2160 mm reference point). Each of these zones serves a distinct function within the deposition process and plays a critical role in determining the thermal, velocity, and radiation characteristics inside the column. Biomass fuels were introduced at the lower section, where combustion initiated the generation of hot gases and radiant energy. These thermal and flow inputs propagated upward through the reaction zone, promoting nanoparticle formation and transport toward the coating surface. The geometric dimensions and boundary conditions of the column were modelled based on the physical parameters shown in the schematic.

Numerical simulations were performed using a CFD-based approach to evaluate the thermal–fluid behaviour across the height of the deposition column. The computational domain was discretised according to the exact geometry shown in **Fig. 1**, ensuring accurate axial alignment between the 0 mm and 2160 mm reference points. The governing equations for mass, momentum, and energy conservation were solved using appropriate turbulence and combustion models, while the Discrete Ordinates (DO) radiation model was used to capture radiative heat transfer. Temperature, velocity, and irradiation data were extracted at multiple axial positions to assess how geometric features such as chamber shape transitions, inlet configurations, and outlet constrictions influence coating conditions. Biomass fuels (PKS, OPF, and EFB) were simulated under identical boundary conditions to compare their combustion performance and its impact on nanoparticle deposition. This methodological framework enabled a systematic evaluation of the combined effects of geometry and fuel type on coating efficiency and thermal uniformity throughout the deposition system.

The schematic diagram presented in **Fig. 1** illustrates the overall geometry and functional layout of the coating deposition column used in this study. The system features a vertically oriented configuration extending from the 0 mm reference point at the base to the 2160 mm reference point at the top, representing the full height of the deposition pathway. Key components of the column include the lower combustion or heating chamber, the central coating or reaction zone, and the upper exhaust or outlet section. The vertical arrangement ensures a controlled upward flow of gases and suspended nanoparticles, allowing the temperature, velocity, and irradiation fields to develop progressively along the column height. This structured environment is essential for generating spatially uniform coating particles and ensuring stable deposition conditions.

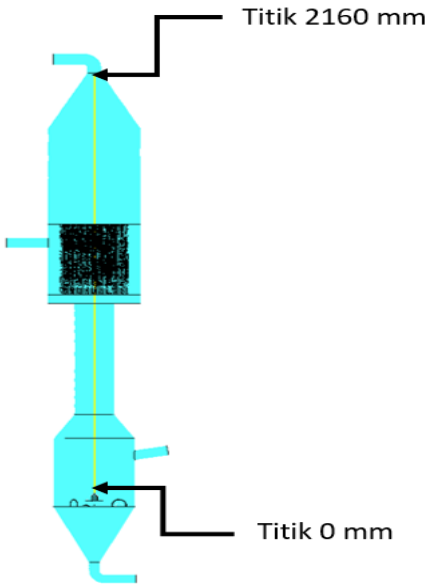

Fig. 1. Schematic Diagram of the Coating Deposition Column

Furthermore, the schematic highlights specific inlets and outlets that facilitate material input, gas flow regulation, and exhaust removal, all of which play a crucial role in the overall thermal–fluid behaviour inside the column. Designating the 0 mm and 2160 mm measurement points provides a clear reference framework for analysing simulation results, enabling temperature, velocity, and irradiation distributions to be correlated with their respective axial positions. This spatial referencing is particularly important for understanding how process variables influence nanoparticle formation, transport, and eventual deposition on target surfaces. Overall, the schematic serves as a foundational representation of the deposition system, guiding both numerical evaluation and experimental interpretation throughout the study.

3. Result & Discussion

The comparative analysis of temperature, velocity, and radiative heat flux distributions presented in Figures 2 through 7 provides a comprehensive understanding of the thermal–fluid behaviour within the coating deposition column under varying geometric configurations and biomass fuel types. These contour evaluations serve as the foundation for assessing how design modifications and combustion characteristics influence nanoparticle formation, transport, and deposition efficiency. By examining the effects of geometry on flow stability, thermal uniformity, and irradiation intensity, as well as the impact of different biomass fuels on heat release and flow momentum, the discussion aims to identify operating conditions that most effectively support high-quality coating performance. The following sections elaborate on these findings, highlighting key differences, trends, and implications for optimising the nanoparticle-based coating process.

The temperature contours in Fig. 2 provide a comparative visualisation of the thermal distribution across the four deposition column geometries. Geometry 1 exhibits a moderate temperature gradient, with temperatures generally ranging from approximately 1800 to 1875 °C. The distribution appears relatively uniform along the column height, indicating stable thermal behaviour but with limited peak temperatures that may constrain nanoparticle activation or coating efficiency. In contrast, Geometry 2 demonstrates a slightly higher temperature field, with values rising to around 1950 °C near the upper section of the reaction zone. This elevated temperature concentration suggests improved thermal energy availability for particle decomposition or coating precursor reactions, although the heating remains localised rather than broadly dispersed throughout the column.

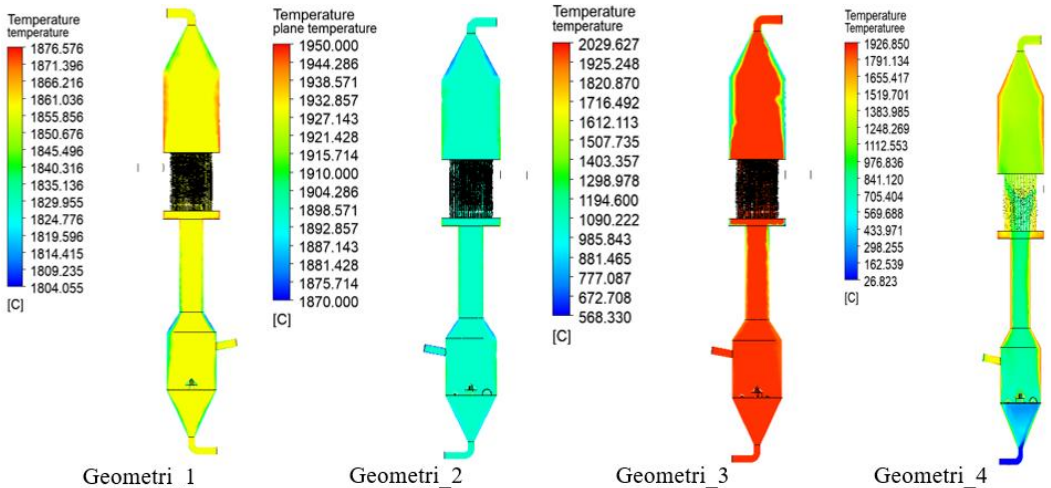

Fig. 2. Comparative Temperature Contours for Deposition Column Geometries (Geometry 1–4)

Geometry 3 presents the highest temperature intensities among all configurations, reaching values exceeding 2020 °C. The temperature field is intensely concentrated around the central coating zone, indicating vigorous thermal activity that may enhance nanoparticle formation and deposition rates.

However, the steep temperature gradient may also induce potential hotspots and risk thermal non-uniformity. Meanwhile, Geometry 4 shows a markedly lower thermal distribution, with temperatures dropping to below 1000 °C in several regions of the column. This geometry demonstrates insufficient heating for effective coating reactions and would likely result in poor nanoparticle adhesion and reduced coating quality. Overall, the thermal comparison across the four geometries reveals that geometric design plays a crucial role in shaping the heat transfer characteristics of the deposition system, directly influencing coating efficiency and uniformity.

The velocity contours presented in **Fig. 3** reveal distinct flow characteristics within the four deposition column geometries. Geometry 1 shows relatively low overall gas velocities, with maximum values around 39 m/s appearing near the upper outlet region. Most of the column maintains velocities below 10 m/s, indicating a stable but slow upward flow of gases. While such low velocities reduce turbulence and promote uniform nanoparticle residence time, they may also limit particle transport efficiency toward the coating zone. Geometry 2, on the other hand, displays moderate velocity intensities, with peaks reaching approximately 20 m/s near the lower combustion chamber and inlet region. The increased flow dynamics in this geometry enhance particle mixing and transport; however, the sharper gradients observed near the base may introduce localised recirculation zones that could affect coating uniformity.

Geometry 3 exhibits the lowest velocity distribution among all configurations, with peak velocities remaining below 0.03 m/s throughout the column. This extremely slow flow suggests inadequate gas momentum and poor particle entrainment, rendering the geometry unsuitable for effective deposition. The lack of velocity-driven upward transport could lead to particle settling and insufficient coating coverage. Conversely, Geometry 4 exhibits a more balanced velocity field, with velocities rising to 20 m/s in localised regions while remaining moderate throughout most of the column height. This geometry likely supports improved particle transport and mixing without inducing excessive turbulence. Collectively, the results indicate that optimal coating performance requires a geometry that provides neither excessively low nor excessively high flow velocities, and Geometry 4 appears to offer the most favourable balance for efficient nanoparticle deposition.

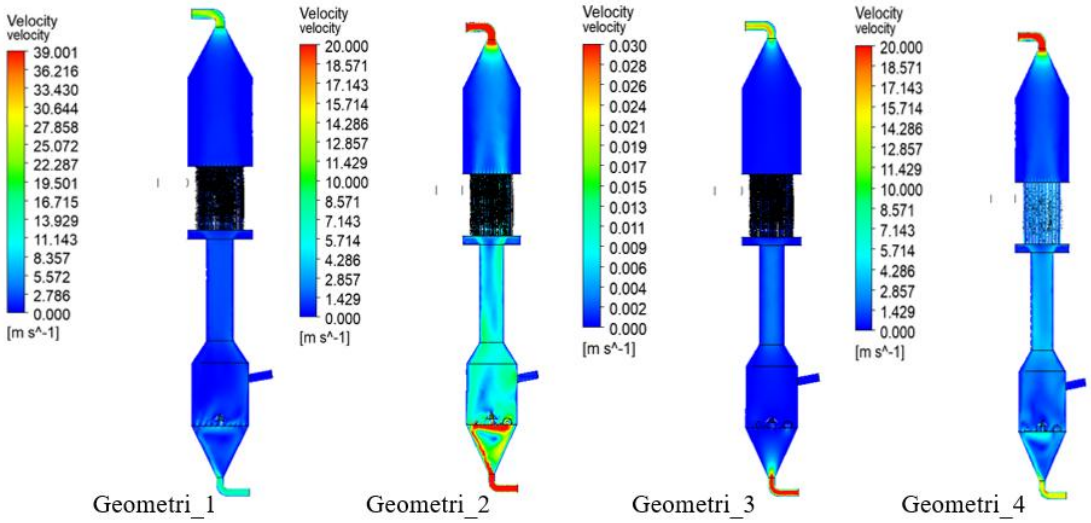

Fig. 3. Comparative Velocity Contours for Deposition Column Geometries (Geometry 1–4)

The DO irradiation contours presented in **Fig. 4** highlight distinct radiative heat flux distributions across the four column geometries. Geometry 1 exhibits moderate irradiation intensities, with values ranging from approximately 1.8×10^3 to 3.3×10^6 W/m². The irradiation is primarily concentrated in the lower region of the column and gradually decreases upward, indicating that radiant energy is not uniformly distributed along the column height. This pattern suggests limited radiative heating in the upper deposition zone, potentially leading to insufficient thermal activation of nanoparticles during the coating process. Geometry 2, however, demonstrates a higher, more uniform irradiation field, with peak values around 3.0×10^6 W/m² across a broader region. The enhanced distribution in this geometry

indicates improved radiative penetration, likely promoting more effective particle heating and facilitating better coating formation.

Geometry 3 shows a further increase in radiative intensity, with maximum irradiation values approaching 3.1 × 10^6 W/m². The irradiation is intensely concentrated around the central coating zone, which may enhance precursor decomposition and nanoparticle formation within this critical region. However, the high concentration could also introduce thermal hotspots and potential overheating, which may negatively affect coating uniformity. In contrast, Geometry 4 presents the highest irradiation intensities, with peak radiative values exceeding 3.4 × 10^6 W/m². While this high radiant energy may significantly improve particle activation and deposition efficiency, the sharp irradiation gradients observed in the upper and lower sections may create non-uniform heating conditions. Overall, the comparison demonstrates that the geometric configuration has a substantial influence on radiative heat transfer within the column, with Geometry 2 and Geometry 3 showing more favourable irradiation distributions for stable, efficient coating processes.

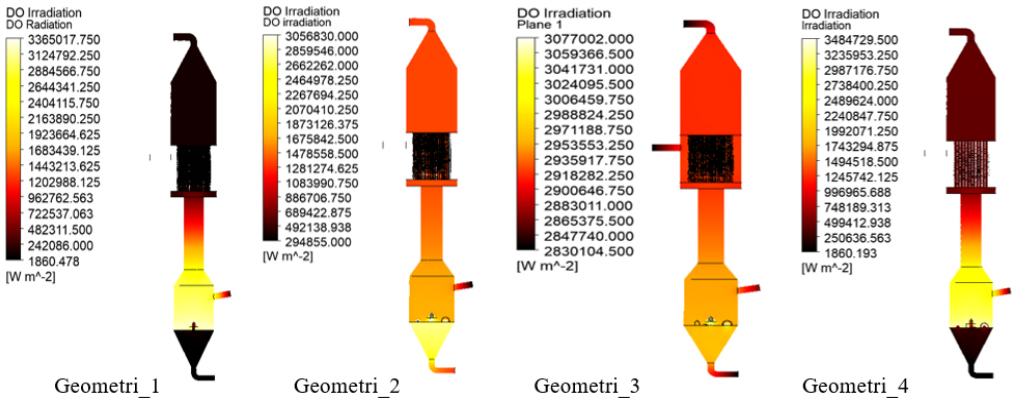

Fig. 4. Comparative DO Irradiation Contours for Deposition Column Geometries (Geometry 1–4)

The temperature contours in **Fig. 5** reveal apparent differences in thermal behaviour among the three biomass fuels: PKS, OPF, and EFB. The combustion of PKS produces a relatively moderate temperature distribution, with peak values reaching approximately 1632 °C. The temperature field is more uniform along the column height, indicating a steady but less intense heat release. This moderate heating may support stable nanoparticle formation but may not provide sufficient thermal energy for rapid precursor decomposition. In comparison, PKS shows a significantly higher temperature field, with peak temperatures exceeding 2051 °C. The elevated temperatures generated by OPF combustion enhance thermal activation, potentially increasing particle synthesis rates and promoting stronger coating adhesion within the deposition zone.

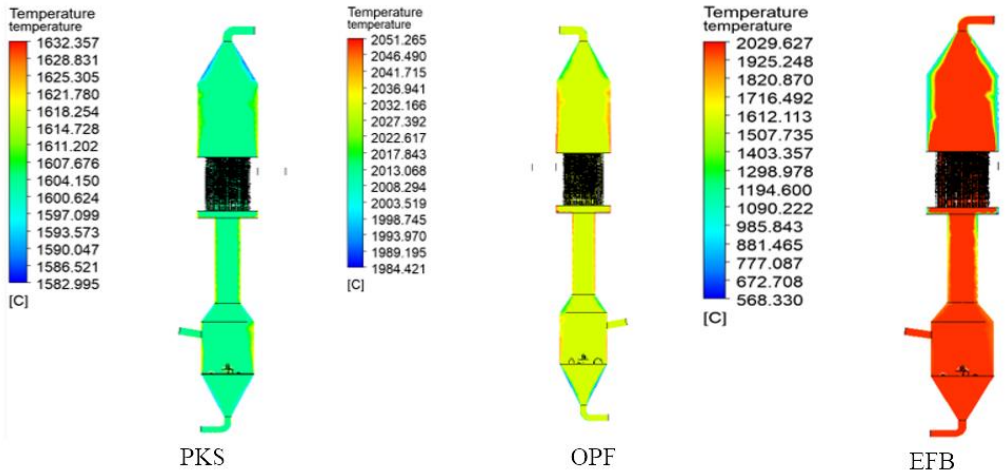

Fig. 5. Comparative Temperature Contours for Biomass Fuels: PKS, OPF, and EFB

EFB exhibits the highest temperature intensities, with maximum values exceeding 2029 °C, but also shows the steepest temperature gradients among the three fuels. The intense heat release, concentrated in the upper and middle regions of the column, suggests vigorous combustion activity, which may accelerate nanoparticle formation but could also introduce thermal nonuniformity and the risk of overheating. Such sharp gradients may lead to inconsistent coating quality unless properly managed by optimising flow and reaction conditions. Overall, the comparative results indicate that OPF and EFB provide higher thermal energy, suitable for efficient nanoparticle deposition, while PKS offers a more controlled, uniform heating profile that may benefit applications requiring gradual or temperature-sensitive coating processes.

The velocity contours in **Fig. 6** indicate that the three biomass fuels, PKS, OPF, and EFB, generate distinct flow behaviours within the deposition column. The combustion of PKS produces relatively low gas velocities, with maximum values remaining below 0.03 m/s across the entire column. This slow, uniform flow suggests a stable flow regime with minimal turbulence, which may support consistent particle residence times but also limit the upward transport of nanoparticles toward the coating region. OPF combustion, on the other hand, yields a slightly more dynamic flow field. Although peak velocities remain modest at around 0.03 m/s, localised areas near the inlet and mid-column show higher velocity gradients, indicating improved mixing and particle entrainment compared to PKS.

In contrast, EFB exhibits the highest velocity intensities among the three fuels, with maximum values reaching approximately 0.05 m/s. The increased velocity field suggests stronger combustion-induced flow momentum, which can enhance particle transport and facilitate more efficient delivery of nanoparticles to the deposition zone. However, steeper velocity gradients may also introduce localised turbulence, potentially affecting coating uniformity. Overall, the comparative analysis demonstrates that EFB offers the most effective momentum for nanoparticle transport, whereas OPF provides moderate and balanced flow conditions. Meanwhile, PKS produces the lowest flow intensities, which may be insufficient for optimal coating performance unless compensated for by adjustments in operating conditions, such as gas flow rate or temperature.

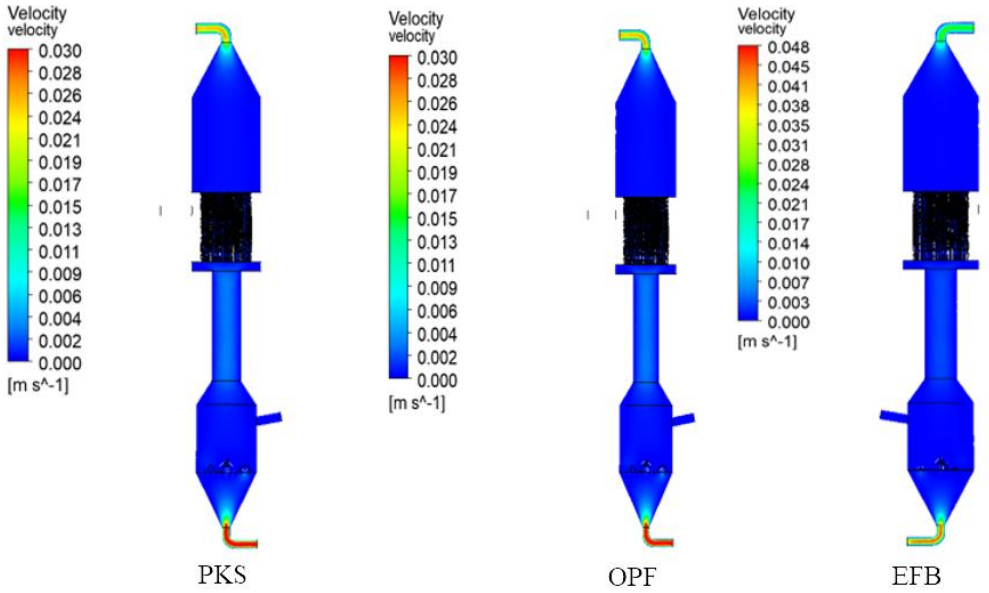

Fig. 6. Comparative Velocity Contours for Biomass Fuels: PKS, OPF, and EFB

The DO irradiation contours presented in **Fig. 7** reveal substantial differences in radiative heat flux generated by the combustion of PKS, OPF, and EFB. The combustion of PKS produces moderate irradiation levels, with values ranging from approximately 2.8×10^6 to 3.0×10^6 W/m². The majority of the radiant energy is concentrated in the middle and lower regions of the column, indicating that radiation heat transfer is relatively balanced but not particularly intense. While this distribution may support stable particle heating, the moderate irradiation levels suggest that PKS combustion may not

provide sufficient radiant energy for high-temperature nanoparticle activation, potentially limiting coating efficiency. In contrast, OPF combustion produces significantly higher irradiance, reaching up to 6.5 × 10^6 W/m². This sharp increase in radiative heat flux indicates stronger combustion-driven radiation, which can substantially elevate particle temperatures and promote rapid precursor decomposition.

EFB demonstrates irradiation patterns of similar magnitude to OPF, with peak radiative values approaching 6.5 × 10^6 W/m². However, the distribution appears more concentrated in the upper section of the column, suggesting that radiation from EFB combustion is more directional and regionally intensified. Such localised irradiation may accelerate particle heating in specific zones but may also lead to thermal non-uniformity within the deposition region. These differences highlight the strong influence of fuel type on the radiative heat-transfer profile within the column. Overall, OPF and EFB exhibit superior radiative performance, which can enhance nanoparticle formation and deposition, while PKS provides a more moderate yet stable irradiation field suitable for controlled or temperature-sensitive coating applications.

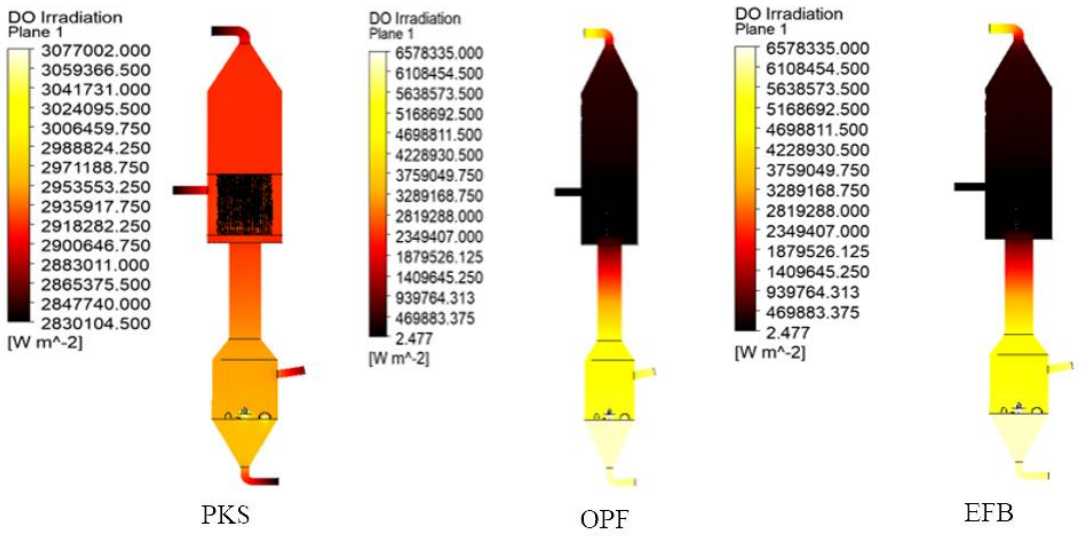

Fig. 7. Comparative DO Irradiation Contours for Biomass Fuels: PKS, OPF, and EFB

The findings of this study demonstrate a significant novelty in understanding how geometric configurations and biomass fuel variations jointly influence the thermal–fluid behaviour within a coating deposition column for nanoparticle-based materials. Unlike previous studies that typically evaluate coating performance using conventional fossil fuels or simplified reactor geometries, this research integrates real biomass combustion profiles with detailed CFD-based assessments of temperature, velocity, and radiative irradiation distributions. The ability to correlate geometric design with the spatial evolution of thermal fields reveals previously unreported insights into how deposition chambers can be optimised to achieve uniform heating, efficient particle entrainment, and enhanced radiative energy transfer. Such an integrated approach provides a more realistic representation of industrial coating environments and offers a new framework for designing energy-efficient and environmentally sustainable deposition systems.

Additionally, the comparative evaluation of three biomass fuels, PKS, OPF, and EFB, introduces a new perspective on the role of alternative renewable energy sources in supporting advanced coating technologies. The identification of OPF and EFB as fuels capable of producing high irradiation flux and favourable velocity dynamics represents an innovative contribution to the field, demonstrating that biomass combustion can be strategically utilised to improve nanoparticle synthesis and coating quality. These findings challenge the conventional assumption that biomass fuels offer inferior thermal performance compared to fossil-based sources, showing that specific biomass types can deliver superior thermal performance when combined with optimised column geometries. This synergy between alternative fuels and system design establishes a new pathway for developing sustainable coating

processes, marking a valuable advancement in both materials engineering and renewable energy applications.

4. Conclusion

This study successfully evaluated the influence of deposition column geometry and biomass fuel type on the thermal–fluid behaviour of a nanoparticle-based coating system through comprehensive CFD simulations that included analyses of temperature, velocity, and radiative heat flux. By modelling the deposition column according to the schematic configuration and applying consistent boundary conditions across four geometric variations and three biomass fuels, the results revealed significant interactions between system design and combustion characteristics. The findings demonstrate that geometric configuration plays a critical role in shaping the distribution of thermal energy, flow momentum, and radiative transfer along the column height. Among the tested designs, Geometry 3 exhibited the most favourable thermal performance due to its high, concentrated temperature field, while Geometry 4 showed improved flow momentum, supporting effective nanoparticle transport. Conversely, Geometry 1 and Geometry 2 provided moderate but more uniform distributions, offering design trade-offs for specific coating requirements.

The comparative assessment of biomass fuels further highlighted the potential of renewable energy sources in high-temperature coating applications. PKS and TKKS produced higher temperatures, stronger radiative heat flux, and more dynamic velocity fields than CKS, indicating their superior suitability for promoting nanoparticle activation and improving deposition efficiency. CKS, while producing lower thermal intensities, provided more stable, uniform heating profiles, which may be advantageous for controlled or temperature-sensitive coating processes. Integrating these insights, the study demonstrates that optimal coating performance can be achieved by selecting a column geometry that balances thermal uniformity with adequate flow momentum and pairing it with biomass fuels that provide high radiative and thermal outputs. Overall, this work offers a new understanding of the synergy between system design and biomass combustion, providing a scientific foundation for developing sustainable, energy-efficient nanoparticle-coating technologies.

Acknowledgement

The authors would like to express their sincere appreciation for the collaborative effort and commitment that made this research possible. This work was fully supported through self-funded contributions from all authors, who collectively provided the financial resources required for computational analysis, data processing, and manuscript preparation. The authors also extend their gratitude to the academic and technical staff who offered valuable insights during the development of the simulation models and interpretation of the results. Their support and constructive feedback greatly enhanced the quality and clarity of this study.

References

El-Sayed, S. A., Mostafa, M. E., Khass, T. M., Noseir, E. H., & Ismail, M. A. (2024). Combustion and mass loss behavior and characteristics of a single biomass pellet positioning at different orientations in a fixed bed reactor. *Biomass Conversion and Biorefinery*, 14(14), 15373–15393.

Erdiwansyah, Gani, A., Zaki, M., Mamat, R., Nizar, M., Rosdi, S. M., … Sarjono, R. E. (2023). Analysis of technological developments and potential of biomass gasification as a viable industrial process: A review. *Case Studies in Chemical and Environmental Engineering*, 8, 100439. Retrieved from https://doi.org/https://doi.org/10.1016/j.cscee.2023.100439

Erdiwansyah, Mahidin, Husin, H., Nasaruddin, Gani, A., & Mamat, R. (2023). Modification of perforated plate in fluidized-bed combustor chamber through computational fluid dynamics

simulation. *Results in Engineering*, 19, 101246. Retrieved from https://doi.org/https://doi.org/10.1016/j.rineng.2023.101246

Erdiwansyah, Mahidin, Mamat, R., Sani, M. S. M., Khoerunnisa, F., & Kadarohman, A. (2019). Target and demand for renewable energy across 10 ASEAN countries by 2040. *The Electricity Journal*, 32(10), 106670. Retrieved from https://doi.org/10.1016/J.TEJ.2019.106670

Erdiwansyah, Mamat, R., Rosdi, S. M., Ghazali, M. F., Rashid, M. I. M., Syahir, A. Z., … Tamimi, A. (2026). A review on AI-enhanced circular energy storage systems for renewable integration. *Energy 360*, 5, 100051. Retrieved from https://doi.org/https://doi.org/10.1016/j.energ.2025.100051

Erdiwansyah, Mamat, R., Sani, M. S. M., & Sudhakar, K. (2019). Renewable energy in Southeast Asia: Policies and recommendations. *Science of The Total Environment*. Retrieved from https://doi.org/https://doi.org/10.1016/j.scitotenv.2019.03.273

Gani, A., Wattimena, Y., Erdiwansyah, Mahidin, Muhibbuddin, & Riza, M. (2021). Simultaneous sulfur dioxide and mercury removal during low-rank coal combustion by natural zeolite. *Heliyon*, 7(5), e07052. Retrieved from https://doi.org/https://doi.org/10.1016/j.heliyon.2021.e07052

Håkansson, A. (2020). On the validity of different methods to estimate breakup frequency from single drop experiments. *Chemical Engineering Science*, 227, 115908. Retrieved from https://doi.org/https://doi.org/10.1016/j.ces.2020.115908

Han, B., Wang, H., Yuan, S., Li, Y., Zhang, X., Lin, D., … Zhu, Y. (2020). Durable and anti-corrosion superhydrophobic coating with bistratal structure prepared by ambient curing. *Progress in Organic Coatings*, 149, 105922. Retrieved from https://doi.org/https://doi.org/10.1016/j.porgcoat.2020.105922

Liu, Y., Liu, X., Hou, J., Li, H. A., Liu, Y., & Chen, Z. (2019). Technical and economic feasibility of a novel heavy oil recovery method: Geothermal energy assisted heavy oil recovery. *Energy*, 181, 853–867. Retrieved from https://doi.org/https://doi.org/10.1016/j.energy.2019.05.207

Mahidin, M., Hamdani, H., Hisbullah, H., Erdiwansyah, E., Muhtadin, M., Faisal, M., … Sidik, N. A. C. (2022). Experimental study on the FBC chamber for analysis of temperature and combustion efficiency using palm oil biomass fuel. *Transactions of the Canadian Society for Mechanical Engineering*, 46(3), 639–649.

Mohanna, H., Honore, D., Gobin, C., Taupin, B., Levy, P., Commandre, J.-M., & Piriou, B. (2021). Experimental and numerical investigation of pulverized biomass flames in a pilot-scale reactor using OH* chemiluminescence imaging and in-flame probing techniques. In *European Biomass Conference and Exhibition (EUBCE 2021)* (pp. 411–424). ETA-Florence Renewable Energies.

Radenahmad, N., Azad, A. T., Saghir, M., Taweekun, J., Bakar, M. S. A., Reza, M. S., & Azad, A. K. (2020). A review on biomass derived syngas for SOFC based combined heat and power application. *Renewable and Sustainable Energy Reviews*, 119, 109560. Retrieved from https://doi.org/https://doi.org/10.1016/j.rser.2019.109560

Rukosuyev, M. V, Barannyk, O., Oshkai, P., & Jun, M. B. G. (2016). Design and application of nanoparticle coating system with decoupled spray generation and deposition control. *Journal of Coatings Technology and Research*, 13(5), 769–779.

Tang, H., Hashigata, K., Chang, T.-F. M., Chen, C.-Y., Nagoshi, T., Yamane, D., … Sone, M. (2018). Sample size effect on micro-mechanical properties of gold electroplated with dense carbon dioxide. *Surface and Coatings Technology*, 350, 1065–1070. Retrieved from https://doi.org/https://doi.org/10.1016/j.surfcoat.2018.02.041

Xing, Y., Zhang, Y., Liu, M., Xu, M., Guo, F., Han, H., … Gui, X. (2019). Improving the floatability of coal with varying surface roughness through hypobaric treatment. *Powder Technology*, 345, 643–648. Retrieved from https://doi.org/https://doi.org/10.1016/j.powtec.2019.01.058

Zheng, Z., Yang, Y., Li, H., Xin, Q., Zhang, S., Liu, Y., … Gao, X. (2020). Effect of multi-pollutant on the catalytic oxidation of dichloromethane over RuO2-WO3/Sn0.2Ti0.8O2 catalyst. *Fuel*, 278, 118207. Retrieved from https://doi.org/https://doi.org/10.1016/j.fuel.2020.118207